RESEARCH PAPER

PCCP
www.rsc.org/pccp

Probing reactive sites within the Photosystem II manganese cluster: Evidence for separate populations of manganese that differ in redox potential

Thomas Kuntzleman,[b] Robert McCarrick,[b] James Penner-Hahn[b] and Charles Yocum*[ab]

[a] *Departments of Molecular, Cellular and Developmental Biology, Ann Arbor MI 48109-1048, USA*
[b] *Department of Chemistry, University of Michigan, Ann Arbor, MI 48109-1048, USA. Fax: +1 734 647 0884; Tel: +1 734 647 0897. E-mail: cyocum@umich.edu*

Received 4th May 2004, Accepted 29th July 2004
First published as an Advance Article on the web 16th September 2004

When the oxygen evolving complex of Photosystem II is depleted of essential cofactor atoms (Ca^{2+} and Cl^{-}) by a high ionic strength treatment that extracts 23 and 17 kDa extrinsic polypeptides, Mn^{2+} can be released by several large reductants (hydroquinone (H_2Q), *N*,*N*,*N*′,*N*′-tetramethyl-*p*-phenylenediamine (TMPD), methyl derivatives of hydroxylamine). This reactivity can be slowed if the enzyme is reconstituted with Ca^{2+}. For TMPD, data from EPR and X-ray absorption spectroscopy indicate that Ca^{2+} reconstitution restricts initial Mn reduction to a site which contains a Mn^{4+} atom. Dimethylhydroxylamine (DMHA), a much smaller Mn reductant, is unable to reduce the cluster under these same conditions, even though DMHA and TMPD can generate Mn^{2+} from the Mn cluster in the absence of Ca^{2+}. These reductants differ in redox potential by about 300 mV, and it is likely that the higher potential reductant, DMHA (+550 mV), is restricted to initially reacting with a Mn^{3+} species that is screened by the Ca^{2+} atom and is incapable, in the presence of Ca^{2+}, of reducing lower potential atoms of the cluster that do react with TMPD. Reduction of the reactive Mn^{3+} species by DMHA in the absence of Ca^{2+}, however, subsequently allows reduction of the remaining 3 Mn. Such an arrangement of metals and potentials in the cluster is in accord with models for the site of water oxidation and for the structure of the Ca–Mn_4 cluster.

Introduction

A tetranuclear Mn cluster comprises part of a catalytic site of Photosystem II (PSII) that oxidizes water to dioxygen. Sequential photon absorptions catalyze the formation of the oxidized Mn ions that participate in water oxidation:

$$2H_2O \rightarrow O_2 + 4H^+ + 4e^-$$

Calcium, Cl^-, and a redox active tyrosine (Y_Z) also participate in this process.[1,2] Collectively, the Mn cluster, Ca^{2+}, Cl^-, and Y_Z make up part of the oxygen-evolving complex (OEC). Binding of Ca^{2+} and Cl^- is regulated by extrinsic polypeptide components of the OEC, which have molecular masses of 17 and 23 kDa.[3–5] Extraction of these polypeptides from PSII by treatment with 2 M NaCl releases Ca^{2+} and Cl^-; addition of these ions to salt-washed PSII centers reconstitutes normal O_2 evolution activity.[3,5] Strontium can occupy the Ca^{2+} binding site and reconstitute O_2 evolution activity, while Cd^{2+}, which also binds tightly to the Ca^{2+} site, fails to restore activity.[6,7] Other mono and divalent cations (Na^+, K^+, Cs^+, Mg^{2+}) have been shown to inhibit PSII by occupying the Ca^{2+} site, but with substantially lower binding affinities than those of Ca^{2+}, Sr^{2+} or Cd^{2+}.[8] Lanthanides also bind to the PSII Ca^{2+} site with high affinity, but these trivalent metals fail to restore O_2 evolution activity.[9,10]

There are five native oxidation states of the OEC that form the catalytic cycle that oxidizes H_2O to O_2. Advancement of the cycle is described by the model of Kok *et al.*, which proposes that the advancement of "S" states of the OEC is catalyzed by absorption of light:[11,12]

$$S_0 \xrightarrow{h\nu} S_1 \xrightarrow{h\nu} S_2 \xrightarrow{h\nu} S_3 \xrightarrow{h\nu} S_4$$

The OEC releases O_2 spontaneously upon formation of S_4, concomitant with reduction of S_4 to the lowest oxidation state, S_0. Upon long-term dark adaptation, all PSII centers relax to the S_1 state. The S_0/S_1 couple has been estimated to be about +700 mV in intact PSII,[13,14] so the OEC must generate about 1 V on each subsequent photon absorption in order for H_2O to be oxidized on the $S_4 \rightarrow S_0$ transition.

Spectroscopic techniques have made important contributions to understanding the roles of the structural and inorganic cofactor components of the OEC. The S_1 state has been extensively characterized owing to its dark stability, which produces a homogeneous population of centers that is amenable to characterization by X-ray absorption spectroscopy (XAS) and electron paramagnetic resonance (EPR). X-Ray absorption near edge structure (XANES) results suggest that the Mn oxidation states in S_1 are $2Mn^{3+}/2Mn^{4+}$.[15,16] Although there is general agreement about this assignment, it is not universally accepted.[17,18] In addition to XANES, extended X-ray absorption fine structure (EXAFS) has provided structural information on S_1. Results of EXAFS experiments indicate that there are three shells of scatterers around Mn, one at 1.8 Å that has been assigned to a combination of Mn–protein and Mn–oxo interactions, one at 2.7 Å that is assigned to Mn–Mn di-μ-oxo bridged interactions and another at 3.3 Å that has been assigned to Mn–Mn alone, or to Mn–Mn and Mn–Ca interaction(s).[19,20] Although the S_1 state is EPR silent in the conventional perpendicular mode, a low field multiline signal can be observed using parallel mode EPR spectroscopy.[21]

Reducing agents that can react with dark adapted PSII have proven useful in providing additional information on the structure and reactivity of the S_1 state. Reduced derivatives of the OEC produced by reactions of PSII with H_2Q and

DOI: 10.1039/b406601d

NH_2OH have been examined by EPR and XAS.[16,22–26] Room temperature EPR spectra of H_2Q treated salt-washed PSII samples that had been reconstituted with Ca^{2+} showed a characteristic Mn six-line signal, whose amplitude was equivalent to about $2Mn^{2+}$ per reaction center.[25] The XANES spectra of these samples were shifted to lower energy, and exhibited the pronounced shoulder that is characteristic of the presence of Mn^{2+}. These results were interpreted to indicate formation of a reduced species with an oxidation state of $2Mn^{2+}/2Mn^{4+}$.[16,25,26] Hydroxylamine treatment produced a very different result; the XANES edge energies were higher (although still lower than those of S_1) and lacked the shoulder produced by H_2Q treatment. Analysis of the edge energies in these samples was interpreted to indicate reduction of Mn^{4+} to Mn^{3+}, to yield an overall OEC oxidation state of $4Mn^{3+}$.[16,26] A comparison of the H_2Q and NH_2OH results provides evidence for discrete sites within the Mn cluster with differing reactivities.

Further evidence for the existence of such sites in the Mn cluster comes from the observation that non-inhibitory amounts of NH_2OH and H_2Q, when added simultaneously to salt washed PSII centers, rapidly inactivate O_2 evolution.[25] Extraction of the 17 and 23 kDa polypeptides is necessary in order for H_2Q to reduce the Mn cluster, and H_2Q–induced inactivation of O_2 evolution activity is slowed substantially by the addition of Ca^{2+}.[25] Studies with NH_2OH and its *N*-methylated derivatives, *N*-methyl hydroxylamine (NMHA) and *N*,*N*-dimethyl hydroxylamine (DMHA), have shown that NH_2OH and NMHA inactivate O_2 evolution in intact PSII membranes whereas DMHA does not. However, it was observed that all three hydroxylamines destroy O_2 evolution in salt-washed PSII.[27] For salt-washed PSII, Cl^- attenuated the inactivation of O_2 evolution induced by NMHA or DMHA, but not by NH_2OH, while Ca^{2+} slowed NH_2OH-induced decay of O_2 evolution in both intact and salt-washed PSII.[28,29]

Although the redox potential of the $S_0 \rightarrow S_1$ transition has been estimated (+700 mV),[13] few experiments to date have attempted to characterize the redox properties of individual Mn atoms in the OEC. The experiments presented here utilize DMHA and TMPD, which differ substantially in their reduction potentials (+550 mV[30] and +235 mV[31] respectively) and their size (Fig. 1), as probes of the redox characteristics of the OEC Mn cluster. Both reagents undergo one electron oxidation to form EPR active radicals (dimethylnitroxide, or $DMNO^{\bullet}$ and $TMPD^{\bullet+}$, respectively). These radicals have been detected by EPR spectroscopy in the reaction of DMHA and TMPD with oxyhemoglobin,[32,33] and $DMNO^{\bullet}$ has been detected in the reaction of DMHA with illuminated, apo-PSII.[34] Our results show that although DMHA is the smaller of the two reductants, Ca^{2+} interferes with its ability to react with OEC Mn. On the other hand, in the presence of Ca^{2+}, TMPD reduces Mn^{4+} to Mn^{3+}, and eventually to Mn^{2+}, but only after long term (24 h) incubations with the reductant. These results are consistent with a model of the OEC in which Ca^{2+} modulates the reactivity of reducing agents with a Mn^{3+} ion whose potential appears to be higher than those of the other atoms in the cluster.

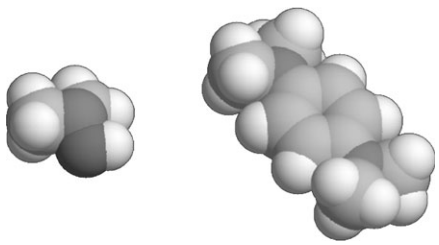

Fig. 1 Space filling models of DMHA ($E^{\circ\prime}$ = +550 mV, left) and TMPD ($E^{\circ\prime}$ = +235 mV, right). Models were created with Chem3D Pro.

Materials and methods

Sample preparation

Photosystem II membranes were isolated from market spinach using the method of Berthold *et al.*[35] with the modifications described in Ghanotakis *et al.*[36] Extraction of the 17 and 23 kDa polypeptides was performed by incubating PSII membranes for 1 h in 2 M NaCl at 0 °C in darkness and then washed twice in a buffer containing 400 mM sucrose, 50 mM MES, and 10 mM NaCl at pH 6.0 (SMN buffer). In order to obtain samples with a high OEC concentration for XANES experiments, reaction center (RCC) preparations (65 chl/PSII) were used; these were isolated as previously described.[37] These highly active preparations (~1200 μmol O_2 (mg Chl)$^{-1}$ h^{-1}) lack the 23 and 17 kDa extrinsic polypeptides as well as light harvesting complexes. All PSII samples were stored in SMN (2–3 mg Chl mL^{-1}) at −70 °C. Samples were assayed for O_2 evolution activity in a buffer containing 50 mM MES (pH 6) and 10 mM $CaCl_2$ (MC buffer) at 25 °C using a Clark-type O_2 electrode, using 350 μM 2,6-dichloro-*p*-benzoquinone as the electron acceptor. Intact PSII preparations gave an activity of 600–700 μmol O_2 (mg Chl)$^{-1}$ h^{-1}; salt washed membranes had activities of 300–400 μmol O_2 (mg Chl)$^{-1}$ h^{-1}.

XANES sample preparation and measurement

XANES samples were incubated with 2 mol of TMPD per mole of PSII reaction center in an ice bucket for 2 h. For experiments with Ca^{2+}-reconsitituted samples, RCC preparations were used. Due to the difficulty in completely depleting RCC preparations of Ca^{2+}, salt washed PSII preparations were used to obtain data on the effects of rigorous Ca^{2+} depletion. At the end of the incubation period, the reaction was quenched with $Fe(CN)_6^{3-}$ and centrifuged at 48 000 *g* for 30 min. The supernatant was discarded and the remaining liquid was removed with an absorbent paper. The pellet was transferred to a lucite XAS cell and covered with a polypropylene film window attached with double faced tape. A blank sample was prepared and showed no Mn contamination.

All XANES experiments were conducted at the Stanford Synchrotron Radiation Laboratory at beam line 7–3, with a Si(220) double crystal monochromator. In order to limit photoreduction, samples were maintained at 10 K using an Oxford Liquid helium flow cryostat. The absence of radiation damage was confirmed by comparing the first and last scans of a sample; in no case was any change observed. Harmonic rejection was achieved by detuning the X-ray beam by 50%. Energy calibration was based on simultaneous measurements of a $KMnO_4$ absorption spectrum, with the pre-edge transition assigned as 6543.3 eV. A Canberra 30 element Ge detector was windowed on the Kα peak of Mn fluorescence for data collection. The data were collected in 5 eV increments in the pre-edge region (6300–6533 eV), 0.2 eV increments over the edge (6533–6552 eV) and 0.6 eV in the post edge region (6552–6586 eV) with integration times of 1 s for the pre- and post-edge regions and 2.5 s for the edge for a total scan time of 15 min scan^{-1}. Each spectrum is the average of eight individual scans.

EPR detection of radicals

EPR samples were prepared from 300 μL aliquots of salt-washed PSII membranes (2–3 mg Chl mL^{-1}) that were supplemented with $Ca(MES)_2$ from a 0.1 M stock solution to bring the final metal concentration to 10 mM. The Cl^- concentration in all samples was kept at 10 mM Cl^-. Reductants were added from 1 mM stock solutions. After addition of DMHA or TMPD, samples were immediately transferred into an aqueous flat cell and $DMNO^{\bullet}$ or $TMPD^{\bullet+}$ EPR signals were measured at room temperature using a Bruker ER-200D spectrometer with a TM cavity operated at X-Band. All procedures were

carried out in the dark. Each signal was scanned once using the following instrument settings: Power, 20 mW; modulation amplitude, 1.25 Gpp; modulation frequency, 100 kHz; sweep width 200 G (DMHA) or 120 G (TMPD); time constant 10 ms; and center field 3480 G. The signal amplitude was determined by measuring the peak to trough amplitude of the center peak of the triplet located at approximately 3465 G (DMHA) or the large, center peak at about 3486 G (TMPD).

Activity inhibition and O_2 evolution assays

Samples were thawed and placed on ice in the dark. In experiments to determine the number of moles of reductant required to inactivate O_2 evolution, Ca^{2+} (if present) was added from a stock solution of freshly prepared 0.1 M $Ca(MES)_2$. Either DMHA or TMPD (0.05–5 mol reductant/mol PSII, assuming 250 Chl/PSII) was added to 100 μL aliquots of the resulting PSII suspension (1.5–3 mg Chl mL^{-1}). Dimethylhydroxylamine was added from a stock solution of 1 mM or 10 mM DMHA/HCl, and TMPD additions were made from freshly prepared solutions of 1 mM or 10 mM TMPD/HCl. The reaction mixtures were incubated in the dark at 4–8 °C for 20–24 h. Results from 48 h incubations gave essentially the same results as 24 h incubations, indicating that the reactions had gone to completion after 24 h. After incubation, samples were assayed for O_2 evolution activity and compared to a control sample that had incubated overnight under the same conditions without reductant. These samples routinely showed $<10\%$ loss in activity and $<10\%$ loss in Mn content (see below). The fraction of centers inactivated was calculated as:

$$F_I = \frac{A_C - A_R}{A_C}$$

where F_I is the fraction of centers inactivated, A_C is the activity of a sample incubated overnight in the absence of reductant, and A_R is the activity of a sample incubated overnight in the presence of reductant.

In experiments comparing the ability of metals to protect the OEC against DMHA inhibition, metals were added from stock solutions of 1 M divalent metal chloride or NaCl. Additions of TMACl were used to maintain the total Cl^- concentration at 30 mM. Samples were incubated in darkness for 24 h at 0 °C in the presence of 4 equivalents of DMHA and then assayed as described above.

Quantitation of Mn loss from PSII

300 μL aliquots of PSII membranes were prepared as described above. After incubation for 24 h under various conditions, 50 mM Ca^{2+} was added to the samples to release adventitiously bound Mn^{2+}.[38] Subsequently, the samples were centrifuged at 12 000 *g* for 20 min. The supernatant was decanted and any residual liquid was absorbed onto tissue; special care was taken to remove any traces of supernatant while maintaining the integrity of the pellet. The pellets were then resuspended to their original 300 μL volume with 0.6 N HCl. Samples were placed in an aqueous flat cell and Mn^{2+} six-line EPR signals were measured at room temperature using a Bruker ER-200D spectrometer with a TM cavity operated at X-Band. Each sample was scanned once using the following instrument settings: Power, 200 mW; modulation amplitude, 10 Gpp; modulation frequency, 100 kHz; sweep width 900 G; time constant 10 ms; and center field was 3480 G. The Mn^{2+} concentration of each sample was determined by comparing the signal amplitudes to a set of standard Mn^{2+} solutions (5–100 μM) in 0.6 N HCl. The fraction of Mn remaining in a pellet was determined by comparing the average signal amplitude of a reductant-treated sample to a control sample incubated without reductant. Typically, samples with no added reductant incubated overnight at 4 °C and then acidified showed less than 10% loss of Mn relative to a sample that was acidified immediately after thawing.

Results

In an ongoing study of the reactivity of the PSII Mn cluster, EPR spectroscopy was utilized to examine the reaction of TMPD with salt-washed PSII membranes. Fig. 2A shows the spectrum observed when two equivalents of TMPD/PSII are mixed and transferred to an EPR flat cell; the spectrum shown was acquired approximately 20 min after mixing. This signal is identical to that previously reported for $TMPD^{\bullet+}$.[32] Photosystem II samples depleted of Mn and then exposed to TMPD showed no EPR signal (data not shown), indicating that TMPD oxidation is due to a reaction between it and the Mn cluster. In Fig. 2B, the development of the radical signal in Ca^{2+} depleted (closed symbols) and Ca^{2+} reconstituted (open symbols) salt-washed PSII samples are shown, demonstrating that the presence of Ca^{2+} slows, but does not block the oxidation of TMPD by reduction of the Mn cluster.

To characterize the effect of Ca^{2+} on the initial site of Mn reduction by TMPD in PSII, reaction center preparations were incubated with TMPD in the presence and absence of Ca^{2+} on ice for 2 h. After centrifugation, the pellet was loaded into an XAS cell and XANES spectra were acquired. Samples depleted of Ca^{2+} and treated with TMPD (Fig. 3A, solid line) show a substantial edge shift to lower energy and a very large shoulder that is clearly indicative of the presence of Mn^{2+},[16] which is absent from the control sample (Fig. 3A, dashed line), whereas PSII samples containing a reconstituted Ca^{2+} site and then exposed to TMPD (Fig. 3B, solid line) exhibit edge energies that are much closer to that of an S_1 edge energy (Fig. 3B, dashed line). The Ca^{2+} reconstituted, TMPD treated samples show a striking similarity to XANES spectra, previously reported for NH_2OH treated PSII samples, which were interpreted to indicate reduction of Mn^{4+} to Mn^{3+}.[16,26] For the Ca^{2+} reconstituted, TMPD treated sample, the edge shift was 0.75 eV. For comparison, a NH_2OH-reducted sample in which $2Mn^{4+}$ were reduced to Mn^{3+}, the edge shift was 1.2 eV.[39] The XANES shift of samples treated with TMPD in the absence of Ca^{2+} (*ca.* 6.5 eV) is comparable to H_2Q treated PSII samples in which reduction of Mn^{3+} to Mn^{2+} was proposed to have occurred.[16,26] A comparison of the data in Fig. 3 with these observations suggests that for TMPD only Mn^{4+} atom(s) are being reduced in the presence of Ca^{2+}, while the Mn^{3+} atoms of the cluster are also being reduced in its absence. This conclusion is consistent with the EPR data (Fig. 2), and both EPR and XANES spectroscopy indicate that Ca^{2+} shields Mn^{3+} atoms of the OEC from reduction by TMPD.

To explore the ability of Ca^{2+} to modulate reduction of the OEC, differences in reactivity of the PSII Mn cluster with DMHA and TMPD were explored. The smaller reductant, DMHA (see Fig. 1), would be expected to have a more facile access to the OEC than the larger TMPD. To test this assumption, formation of the $DMNO^{\bullet}$ radical, produced as a result of the dark reaction of salt-washed PSII centers with DMHA, was monitored by EPR spectroscopy. Oxidation of DMHA by illuminated, apo-PSII has been reported previously.[34] Fig. 4 shows the EPR spectrum that is observed when two moles of DMHA per mole PSII were added to Ca^{2+} deficient, salt-washed PSII centers and transferred immediately to an EPR flat cell (top trace). The EPR signal shown here is identical to signals that have been assigned to the $DMNO^{\bullet}$ radical.[33] In contrast to the reaction between TMPD and PSII, addition of 10 mM Ca^{2+} to these samples prior to addition of DMHA drastically attenuated the production of the radical (Fig. 4, bottom trace), whereas samples containing 10 mM Na^+ in place of Ca^{2+} showed rapid development of the radical. Addition of Sr^{2+} and Cd^{2+} blocked radical formation, while

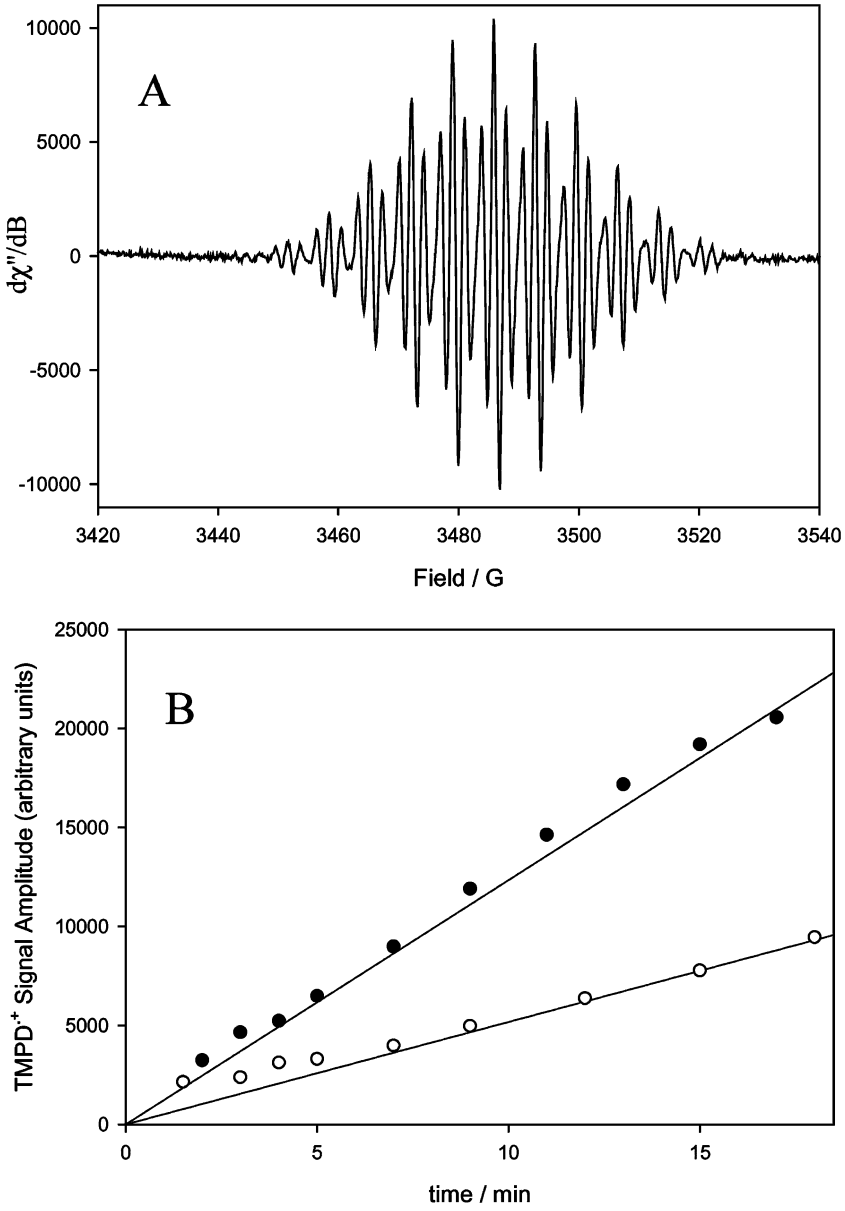

Fig. 2 Effect of Ca^{2+} on $TMPD^{\bullet+}$ formation by salt-washed PSII incubated with 2 mol of TMPD per mole PSII in the dark in the presence of 10 mM Cl^-. (A) An EPR spectrum of the radical formed in the reaction between salt-washed PSII and TMPD in the absence of added Ca^{2+}; (B) Effect of Ca^{2+} on radical formation. Closed symbols, minus Ca^{2+}, open symbols, reconstituted with 10 mM Ca^{2+}. At 20 min, the radical signal amplitudes correspond to 16.2 μM $TMPD^{\bullet+}$ ($-Ca^{2+}$) and 8.1 μM $TMPD^{\bullet+}$ ($+Ca^{2+}$), which correspond to 1.2 and 0.6 TMPD oxidized per PSII reaction center.

Mg^{2+} addition did not (data not shown), indicating that the reaction between DMHA and OEC Mn is prevented when the Ca^{2+} site is reconstituted with an appropriate metal.

The loss of O_2 evolution in salt-washed PSII following treatment with DMHA was monitored to further characterize the interaction of DMHA with the PSII OEC in the dark. Photosystem II centers were incubated with stoichiometric amounts of DMHA at 4 °C in darkness for 24 h and samples were subsequently assayed in MC buffer. Fig. 5A shows the effect of increasing concentrations of DMHA on O_2 evolving activity in salt-washed PSII centers. In the absence of added Ca^{2+}, inactivation of O_2 evolution appears to saturate at 2–3 moles of DMHA/mole PSII (Fig. 5A, closed symbols). However, samples incubated in the presence of 10 mM Ca^{2+} showed little loss of activity due to DMHA treatment (Fig. 5A, open symbols). Additionally, Sr^{2+} and Cd^{2+} prevented the loss of O_2 evolution caused by DMHA, whereas weakly binding ions (Mg^{2+} and Na^+) were ineffective in protecting against loss of O_2 evolution (Fig. 5B). Thus, Ca^{2+} and those metals that compete effectively with it for binding to PSII conferred protection against DMHA inactivation of the OEC, apparently by blocking the ability of DMHA to react with Mn.

In order to more specifically determine the site of DMHA reactivity within the OEC, Mn^{2+} release from salt-washed PSII treated with DMHA was quantified. Salt-washed PSII samples were incubated in the dark for 24 h at 4 °C with increasing amounts of DMHA. After 24 h, a high concentration (50 mM) of Ca^{2+} was added to displace any adventitiously bound Mn^{2+},[38] the samples were centrifuged and the pellets were acidified. The resulting Mn^{2+} from the pellet was measured by EPR. In salt-washed PSII samples not reconstituted with Ca^{2+} prior to reductant exposure, Mn release reached a maximum at 6 mol DMHA/mol PSII (Fig. 6, closed symbols). When a saturating concentration of DMHA was added, approximately 75% of the Mn was released, corresponding to 3 out of 4 Mn, which indicates that DMHA reduces PSII Mn to Mn^{2+} in darkness in the absence of Ca^{2+}. The release of Mn^{2+} was biphasic with respect to the amount of reductant added; ~50% of the Mn was reduced and released by the first two mol DMHA/mol PSII and the next 25% of the Mn was

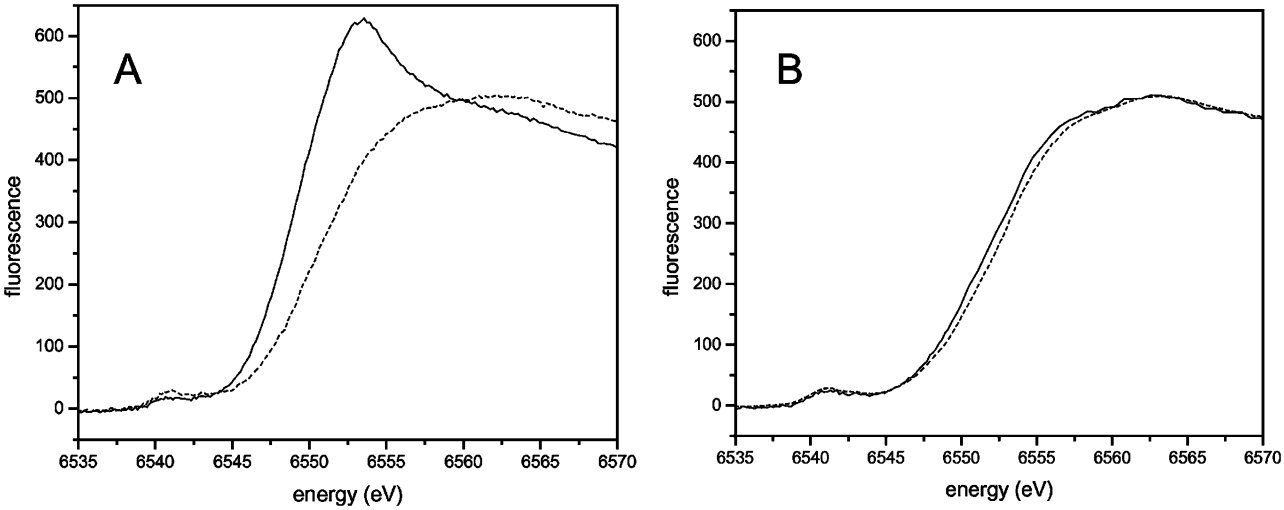

Fig. 3 Characterization by XANES spectroscopy of the effect of Ca^{2+} on TMPD reduction of the PSII Mn cluster. (A) XANES spectra of Ca^{2+} depleted salt washed PSII incubated for 2 h with 2 mol of TMPD per mole PSII. This sample had lost 40% of its activity prior to centrifugation and loading into an XAS cell; (B) Reaction centers reconstituted with 10 mM Ca^{2+} and incubated with TMPD under the same conditions as (A). This sample exhibited no detectable loss of activity.

extracted by addition of the next four mol DMHA/mol PSII. These results could arise from a series of reactions in which one DMHA must first reduce and release one Mn, opening a second Mn to rapid reduction and release. These two reductions would subsequently allow four DMHA react slowly with the remaining Mn, releasing one of the remaining two metals. However, if samples were reconstituted with 10 mM Ca^{2+} prior to the reductant incubations, the PSII centers retained >85% of control levels of Mn, even at the highest DMHA concentrations (>10 mol (mol PSII)$^{-1}$, data not shown) used in these experiments, demonstrating that reduction of the Mn cluster by DMHA was blocked in these samples.

A comparison of the effects on activity of long-term (24 h) incubation of Ca^{2+} reconstituted, salt-washed PSII samples with TMPD and DMHA was also carried out. The results are shown in Fig. 7, which presents data obtained with increasing concentrations of both reductants. For DMHA, minimal activity loss was incurred, as expected (see Fig. 5). In contrast to the results of 2 h exposure of such samples to TMPD (Fig. 3B), where losses of activity were not detected, the long term incubation experiments yielded inhibitions of >90%. Under these conditions, long term incubation with TMPD also resulted in a loss of Mn (data not shown). The ability of Ca^{2+} to prevent a small reductant (DMHA) from reacting with OEC Mn, even under conditions such those shown in Fig. 7, is difficult to reconcile with data showing that under identical conditions, a much larger reductant (TMPD) can inhibit the OEC and reduce and release Mn. Because this is the case, thermodynamic, rather than kinetic factors are likely to be responsible for the differences in reactivity of these compounds, and the difference in redox potentials between DMHA and TMPD may account for the difference in reactivity.

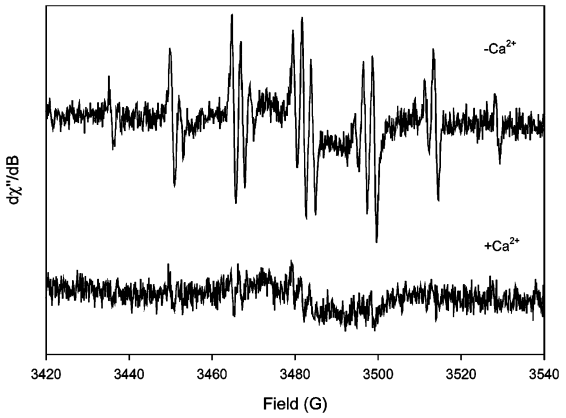

Fig. 4 Effect of Ca^{2+} on $DMNO^{\bullet}$ formation by salt-washed PSII incubated with 2 moles of DMHA per mole PSII in the dark in the presence of 10 mM Cl^{-}. (Top) An EPR Spectrum of the radical formed in the reaction of salt-washed PSII with DMHA in the absence of added Ca^{2+}; (Bottom) An EPR spectrum of the radical formed in the reaction of salt-washed PSII with DMHA in the presence of added Ca^{2+}.

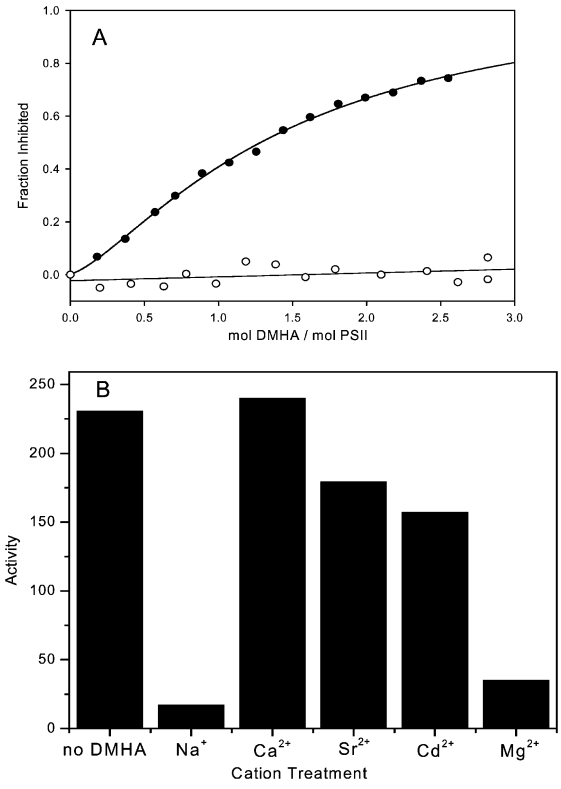

Fig. 5 (A) Inhibition of O_2 evolution in salt-washed PSII as a result of incubation with DMHA for 24 h in the dark at 4 °C. Closed symbols, a sample incubated with 10 mM NaCl; open symbols, incubated with 10 mM $Ca(MES)_2$ and 10 mM NaCl: (B) Effect of cations on loss of O_2 evolution activity by salt-washed PSII incubated for 24 h in the presence of 4 equivalents of DMHA, 10 mM cation, 20 mM Na^{+} and 30 mM Cl^{-}.

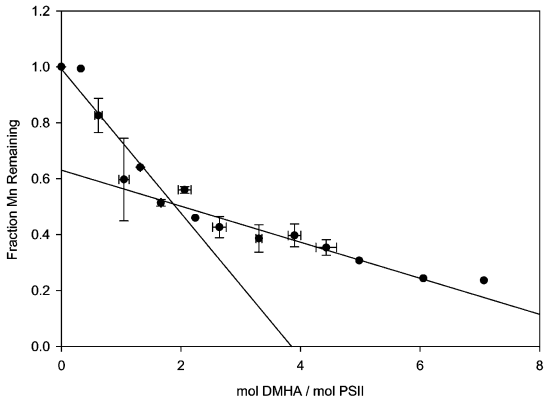

Fig. 6 Mn^{2+} release from salt-washed PSII after a 24 h dark incubation with DMHA. At the end of the incubation period, 50 mM Ca^{2+} was added to the samples to displace any adventitiously bound Mn^{2+}, followed by centrifugation, resuspension and acidification with 0.6 M HCl. The lines represent linear fits of the data from additions of 0–2 mol and 2–6 mol DMHA, respectively.

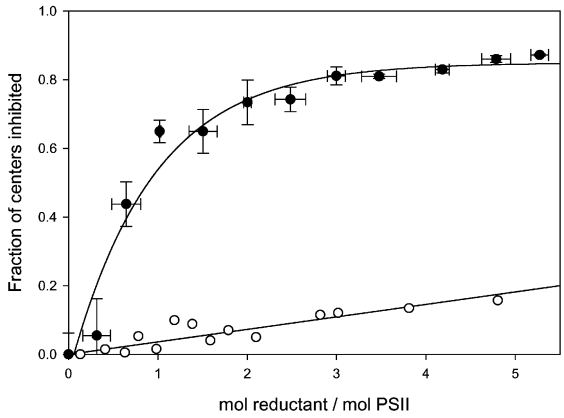

Fig. 7 Inhibition of O_2 evolution in salt-washed PSII as a function of moles of reductant added. Samples incubated for 24 h in the dark at 4 °C, pH 6, in the presence of 10 mM NaCl and 10 mM $Ca(MES)_2$. Closed symbols, TMPD; open symbols, DMHA.

Discussion

Earlier experiments that probed the PSII OEC with NH_2OH and H_2Q demonstrated that the Mn cluster exhibits differential reactivity with respect to reductant identity.[16,25,26] In the experiments presented here, DMHA and TMPD, reductants with different redox potentials and size, also yielded very different results in terms of their effect on the OEC. In the absence of Ca^{2+}, loss of O_2 evolution activity and release of Mn^{2+} was observed in salt-washed PSII samples incubated with DMHA. This, together with the observation that DMNO• radicals are formed, indicates that DMHA can react with and reduce the Mn cluster, releasing Mn^{2+} in the process. The release of Mn^{2+} was biphasic with respect to the concentration of DMHA present. About 2 Mn/PSII were released upon exposure to the first 2 mol DMHA and an additional 1 Mn/PSII was released when the next 4 mol DMHA are added. These Mn^{2+} release data are indicative of a process in which one DMHA can react rapidly with the Mn cluster,

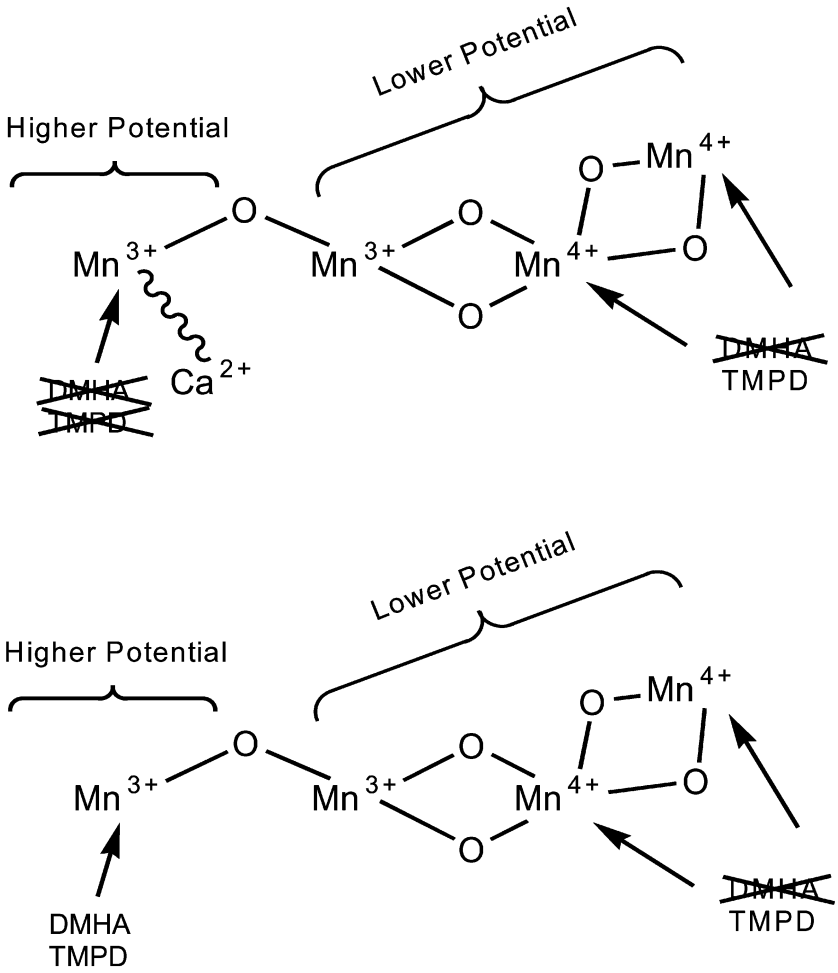

Fig. 8 A schematic model for the relative positions of Mn and Ca^{2+} atoms in the OEC derived from the differential reactivities of Mn atoms with DMHA and TMPD. On the basis of the results presented here, Ca^{2+} is like to be situated so as to screen a high potential Mn^{3+} atom from attack by exogenous reductants such as DMHA and TMPD.

releasing one Mn^{2+}, and exposing a second Mn to fast reduction by another DMHA. Subsequently, another four DMHA react more slowly, releasing one additional Mn^{2+}. The following series of reactions is proposed to account for the Mn^{2+} release data and EPR detection of the $DMNO^{\bullet}$ radical in the reaction between salt-washed PSII and DMHA:

1 DMHA + 1 Mn^{3+} → 1 Mn^{2+} released + 1 $DMNO^{\bullet}$ (fast)
1 DMHA + 1 Mn^{3+} → 1 Mn^{2+} released + 1 $DMNO^{\bullet}$ (very fast)
4 DMHA + 2 Mn^{4+} → 1 Mn^{2+} bound + 1 Mn^{2+} free + 4 $DMNO^{\bullet}$ (slow)

In the presence of Ca^{2+}, the reaction of DMHA with the Mn cluster was strongly inhibited. Loss of O_2 evolution and Mn^{2+} release did not occur when DMHA was added to salt-washed PSII samples incubated in the presence of Ca^{2+}, and room temperature EPR experiments failed to detect the $DMNO^{\bullet}$ radical. These same experiments yielded similar results when Ca^{2+} was replaced by Sr^{2+} or Cd^{2+}, both of which are known to bind to the Ca^{2+} site.[8] However, Na^{+} and Mg^{2+}, which do not bind with high affinity at the Ca^{2+} site, failed to protect against DMHA inactivation, providing further evidence that the Ca^{2+} site in PSII regulates access of reductants to one site in the OEC Mn cluster.

Like DMHA, TMPD has been observed to cause loss of activity and Mn^{2+} (data not shown) in salt-washed PSII centers. However, in Ca^{2+} reconstituted samples, the reduction of the Mn cluster by TMPD was slowed, but not blocked, indicating that TMPD can react at a site that is inaccessible to DMHA in the presence of Ca^{2+}. A comparison of the XANES spectra obtained from samples treated with TMPD for 2 h (Fig. 3) with spectra obtained from NH_2OH and H_2Q treated PSII[16,26] indicates that TMPD reduces only Mn^{4+} in the presence of Ca^{2+} but is also able to reduce Mn^{3+} in its absence.

The differences in reactivity with OEC Mn exhibited by TMPD and DMHA are not consistent with steric factors associated with the different sizes of these reductants. Thus, the difference in reactivity is probably due to the lower redox potential of TMPD. This, in turn, suggests that there are two sites in the Mn cluster that differ in redox potential: a higher potential, Ca^{2+}-sensitive site capable of oxidizing both DMHA and TMPD and a lower potential Ca^{2+} insensitive site that can oxidize TMPD, but not DMHA. Because DMHA appears to react first with a Mn^{3+} in the absence of Ca^{2+}, but cannot reduce Mn in the presence of Ca^{2+}, it is likely that Ca^{2+} occupies a site that restricts access to one or both Mn^{3+}. The model shown in Fig. 8 presents a schematic representation of the positions of the Mn and Ca^{2+} atoms of the OEC arranged according to the effect of Ca^{2+} on initial accessibility of TMPD and DMHA to the metal center. Under conditions that employ a two h incubation period, reduction of Mn^{3+} by TMPD occurs only when Ca^{2+} is absent. Therefore, it is possible that Ca^{2+} either restricts access to the high potential Mn^{3+} site or, alternatively, stabilizes the site such that electron transfer cannot occur. In the absence of Ca^{2+}, it is difficult to determine whether a Mn^{3+} or Mn^{4+} is the first species to be reduced by TMPD.

Three X-ray crystal structures of PSII are currently available,[40–42] each of which presents the Mn cluster as a trimer-monomer arrangement. The most recent structure[42] also contains the most detailed model of the metal center, and predicts that this site is a cubane-like Mn_3Ca structure with the fourth Mn atom placed so as to form an approximate monomer–trimer arrangement with respect to the remaining Mn atoms of the cluster. The monomeric Mn atom and the Ca^{2+} atom are suggested to constitute the active site of water oxidation, following models which suggest that Ca^{2+} ligates a substrate water that forms the O–O bond with a second, Mn^{5+}=O species formed by the conversion of S_3 to S_4.[43,44] The model we present here is consistent topologically with those models in that it predicts that access by water to its site of oxidation in the OEC is affected by the Ca^{2+} atom that is part of the metal cluster, consistent with an earlier model derived from reductant probing experiments with NH_2OH.[29] The difference in redox activity within the Mn cluster may simply be a consequence of the oxidation states and ligand environments of the Mn^{4+} atoms of the cluster. These metals are predicted to be ligated by oxo anions derived from either oxo bridges or acidic amino acid residues.[41] In the case of the Mn^{4+} atoms in the OEC, this type of ligation would be expected to stabilize the metals against reduction, and this, in turn, may account for their lack of reactivity in the case of DMHA.

Acknowledgements

This research was supported by grants from the Photosynthesis Program of the National Research Initiative Competitive Grants Program of the USDA (99-35306-7613) and the National Science Foundation Grant (MCB 0110455) to CFY, and by a grant from the National Institutes of Health (R01-GM-045205) to JEPH. TK was supported by a research training grant in Molecular Biophysics funded by NIH (T32-GM008270.

References

1 T. M. Bricker and D. F. Ghanotakis, in *Introduction to Oxygen Evolution and the Oxygen-Evolving Complex, Oxygenic Photosynthesis: The Light Reactions*, ed. D. R. Ort and C. F. Yocum, Kluwer Academic Publishers, Dordrecht, The Netherlands, 1996, pp. 113–136.
2 R. D. Britt, in *Oxygen, Oxygenic Photosynthesis: The Light Reactions*, ed. D. R. Ort and C. F. Yocum, Kluwer Academic Publishers, Dordrecht, The Netherlands, 1996, vol. 4, pp. 137–164.
3 M. Miyao and N. Murata, *FEBS. Lett.*, 1985, **180**, 303–308.
4 M. Miyao, Y. Fujimura and N. Murata, *Biochim. Biophys. Acta*, 1988, **936**, 465–474.
5 M. Miyao and N. Murata, *FEBS Lett.*, 1984, **168**, 118–120.
6 D. F. Ghanotakis, G. T. Babcock and C. F. Yocum, *FEBS. Lett.*, 1984, **167**, 127–130.
7 C. M. Waggoner and C. F. Yocum, in *Current Research in Photosynthesis*, ed. M. Baltscheffsky, Kluwer, Dordrecht, The Netherlands, 1985, pp. 733–736.
8 J. Vrettos, D. Stone and G. W. Brudvig, *Biochemistry*, 2001, **40**, 7937–7945.
9 D. F. Ghanotakis, G. T. Babcock and C. F. Yocum, *Biochim. Biophys. Acta*, 1985, **809**, 173–180.
10 T.-A. Ono, *J. Inorg. Biochem*, 2000, **82**, 85–91.
11 B. Kok, B. Forbush and M. McGloin, *Photochem. Photobiol.*, 1970, **11**, 457–475.
12 B. Forbush, B. Kok and M. McGloin, *Photochem. Photobiol.*, 1971, **14**, 307–321.
13 I. Vass and S. Styring, *Biochemistry*, 1991, **30**, 830–839.
14 C. Tommos and G. T. Babcock, *Biochim. Biophys. Acta*, 2000, **1458**, 199–219.
15 V. Yachandra, K. Sauer and M. Klein, *Chem. Rev.*, 1996, **96**, 2927–2950.
16 P. Riggs, R. Mei, C. F. Yocum and J. E. Penner-Hahn, *J. Am. Chem. Soc.*, 1992, **114**, 10650–10651.
17 G. C. Dismukes and Y. Siderer, *Proc. Natl. Acad. Sci. USA*, 1981, **78**, 274–278.
18 M. Zheng and G. C. Dismukes, in *Research in Photosynthesis*, ed. N. Murata, Kluwer Academic Publishers, Dordrecht, The Netherlands, 1992, pp. 305–308.
19 V. K. Yachandra, R. Guiles, A. McDermott, J. Cole, R. D. Britt, S. Dexheimer, K. Sauer and M. P. Klein, *Biochemistry*, 1987, **30**, 830–839.
20 J. E. Penner-Hahn, J. Fronko, V. L. Pecoraro, C. F. Yocum, S. D. Betts and N. R. Bowlby, *J. Am. Chem. Soc.*, 1990, **112**, 2549–2557.
21 K. Campbell, J. Peloquin, D. Pham, R. J. Debus and R. D. Britt, *J. Am. Chem. Soc.*, 1998, **120**, 447–448.
22 J. H. A. Nugent, I. Muhiuddin and M. C. W. Evans, *Biochemistry*, 2003, **42**, 5500–5507.
23 J. Messinger, J. H. A. Nugent and M. C. W. Evans, *Biochemistry*, 1997, **36**, 11055–11060.

24 J. Messinger, J. Roblee, O. Wa, K. Sauer, V. K. Yachandra and M. P. Klein, *J. Am. Chem. Soc*., 1997, **119**, 1349–1350.
25 R. Mei and C. F. Yocum, *Biochemistry*, 1992, **31**, 8449–8454.
26 P. Riggs-Gelasco, R. Mei, C. F. Yocum and J. E. Penner-Hahn, *J. Am. Chem. Soc*., 1996, **118**, 2387–2399.
27 R. Mei and C. F. Yocum, *Photosynthesis Research*, 1993, **38** 449–453.
28 R. Mei and C. F. Yocum, *Biochemistry*, 1991, **30**, 7836–7842.
29 K. A. Vander Meulen, A. Hobson and C. F. Yocum, *Biochemistry*, 2002, **41**, 958–966.
30 A. M. Prokai and R. K. Ravichandran, *J. Chromatogr. A*, 1994, **667**, 298–203.
31 N. Leventis and X. Gao, *J. Electroanal. Chem*., 2001, **500** 78–94.
32 C. Storle, K. Stettmeier and P. Eyer, *Free Radical Res. Commun*., 1992, **17**, 133–141.
33 K. Stolze and H. Nohl, *Free Radical Res. Commun*., 1990, **8** 123–131.
34 W. Beck and G. Brudvig, *Biochemistry*, 1987, **26**, 8285–8295.
35 D. A. Berthold, G. T. Babcock and C. F. Yocum, *FEBS. Lett*., 1981, **134**, 231–234.
36 D. Ghanotakis, J. Topper, G. T. Babcock and C. F. Yocum, *Biochim. Biophys. Acta*, 1984, **767**, 524–531.
37 D. F. Ghanotakis, D. M. Demetriou and C. F. Yocum, *Biochim. Biophys. Acta*, 1987, **891**, 15–21.
38 C. F. Yocum, C. T. Yerkes, R. R. Sharp, R. E. Blankenship and G. T. Babcock, *Proc. Natl. Acad. Sci. USA*, 1981, **78**, 7507–7511.
39 P. S. DeMarois, PhD Thesis, University of Michigan, 1999, p. 35.
40 A. Zouni, H. T. Witt, J. Kern, P. Fromme, N. Krauss, W. Saenger and P. Orth, *Nature*, 2001, **409**, 739–743.
41 N. Kamiya and J. Shen, *Proc. Nat. Acad. Sci. USA*, 2003, **100** 98–103.
42 K. Ferreira, T. Iverson, K. Maghlaoui, J. Barber and S. Iwata, *Science*, 2004, **303**, 1831–1838.
43 J. Vrettros, J. Limburg and G. W. Brudvig, *Biochim. Biophys. Acta*, 2001, **1503**, 229–245.
44 V. L. Pecoraro, M. Baldwin, M. Caudle, W. Hsieh and N. Law, *Pure Appl. Chem*., 1998, **70**, 925–929.

